Closed-Loop Control of Functional Neuromuscular Stimulation

NIH Neuroprosthesis Program Contract Number N01-NS-6-2338
Quarterly Progress Report #13
April 1, 1999 to June 30, 1999

Investigators:
Patrick E. Crago, Ph.D.
Clayton L. Van Doren, Ph.D.
Warren M. Grill, Ph.D.
Michael W. Keith, M.D.
Kevin L. Kilgore, Ph.D.
Joseph M. Mansour, Ph.D.
Wendy M. Murray, PhD.
P. Hunter Peckham, Ph.D.
David L. Wilson, Ph.D.

Cleveland FES Center

Departments of Biomedical Engineering,
Mechanical and Aerospace Engineering,
and Orthopaedics
Case Western Reserve University
and MetroHealth Medical Center

1. SYNTHESIS OF UPPER EXTREMITY FUNCTION

The overall goals of this project are (1) to measure the biomechanical properties of the neuroprosthesis user's upper extremity and incorporate those measurements into a complete model with robust predictive capability, and (2) to use the predictions of the model to improve the grasp output of the hand neuroprosthesis for individual users.

1. a. BIOMECHANICAL MODELING: PARAMETERIZATION AND VALIDATION

Purpose

In this section of the contract, we will develop methods for obtaining biomechanical data from individual persons. Individualized data will form the basis for model-assisted implementation of upper extremity FNS. Using individualized biomechanical models, specific treatment procedures will be evaluated for individuals. The person-specific parameters of interest are tendon moment arms and lines of action, passive moments, and maximum active joint moments. Passive moments will be decomposed into components arising from stiffness inherent to a joint and from passive stretching of muscle-tendon units that cross one or more joints.

Progress Report

1. a. i. MOMENT ARMS VIA MAGNETIC RESONANCE IMAGING

Abstract

The outcome of ECU to ECRB tendon transfer surgery was simulated using experimental and modeling tools that can be applied to specific individuals. The moment-angle properties of the Extensor Carpi Ulnaris (ECU) were measured during electrical stimulation, and the tendon moment arm- angle relationships of the ECU and Extensor Carpi Radialis Brevis (ECRB) were estimated from 3D MRI data. With the moment-angle and moment arm-angle relationships the force-excursion property of the ECU was characterized. The ECU was found to be acting on the descending limb of its force-excursion curve over a significant portion of the angular range of motion. The ECU to ECRB tendon transfer was then simulated using the force-excursion properties of the ECU with the moment arm of the ECRB. Simulations predict that the ECU after transfer produces a wrist extension that is smaller than the ulnar deviation moment produced before transfer, and the ECU acts close to the plateau of it's force-excursion curve, thus the optimal transfer is without a change in muscle length when the wrist is in a neutral posture. The predicted values have 15% coefficient of variation for errors associated with measurements and are most sensitive to moment arm measurement errors.

Progress Report

Introduction

Individuals with C5 level tetraplegia lose control of their hand muscles and their wrist extensors. Individuals with C6 level tetraplegia may have some radial wrist extensors like Extensor Carpi Radialis Longus or Brevis (ECRL or ECRB), but they are often weakened due to lower motor neuron damage [Pedretti et al. 1990]. This limits the voluntary wrist extension possible. Voluntary wrist extension can be strengthened or wrist extension can be added by a surgical tendon transfer procedure. The tendon of a voluntary muscle like the Brachioradialis (BR), or a paralyzed but innervated muscle like the Extensor Carpi Ulnaris (ECU) is detached near its insertion, moved over and sutured into the tendon of a primary wrist extensor like the ECRL or ECRB [Freehafer et al. 1992, Keith et al.1996]. The extension at the wrist is the sum of residual voluntary extension, extension due to transfer of a voluntary muscle and extension due to a stimulated transfer, as may be the case [Adamcyzk et al. 1999].

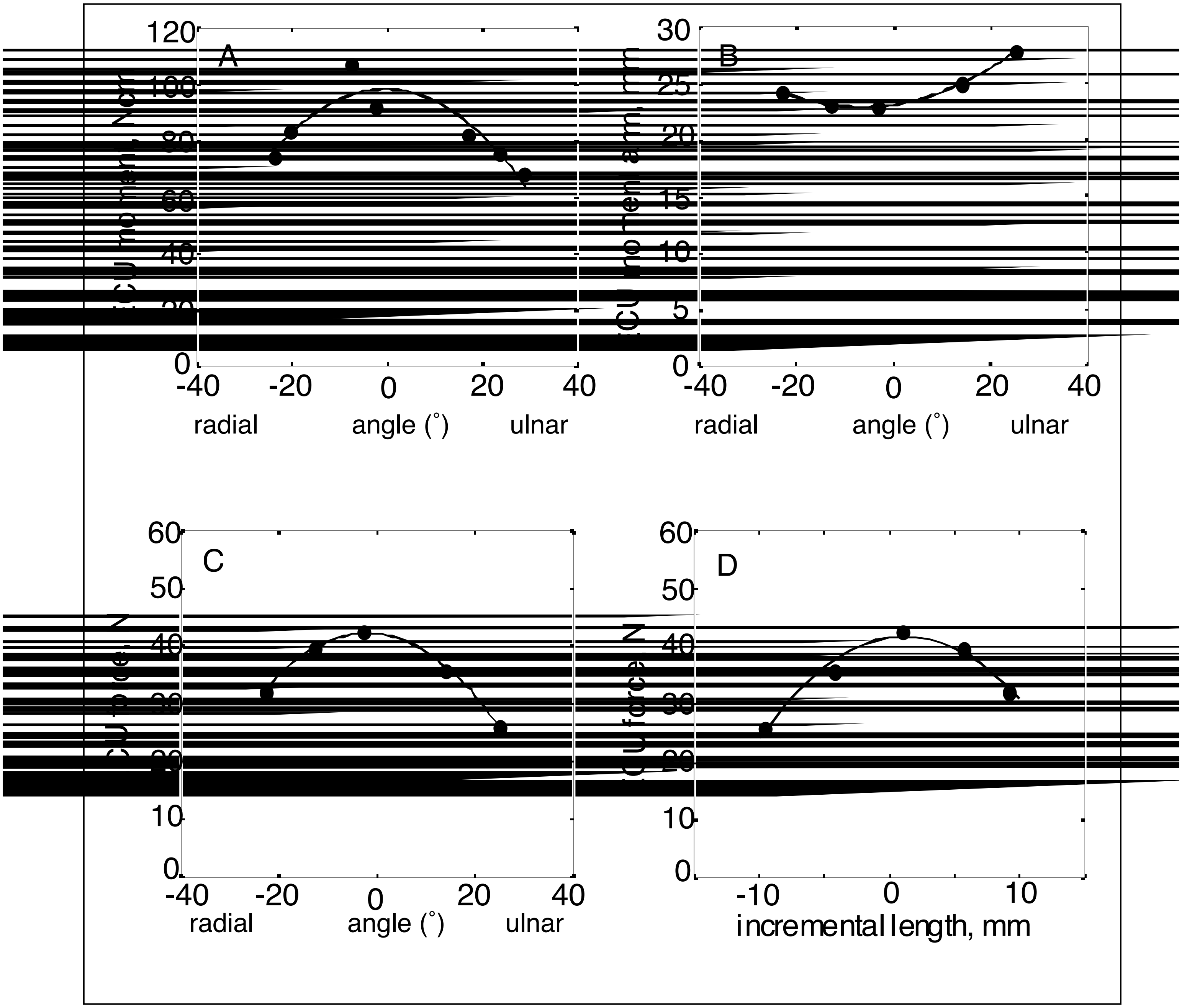

Figure 1.a.i.1. A) Wrist moment due to ECU stimulation as a function of wrist radial-ulnar angle. Data is fit with a quadratic equation $y = -0.0230 \cdot x^2 + 0.7575 \cdot x + 76.8435$. B) ECU moment arm as a function of radial-ulnar angle. Quadratic fit $y = -0.0031 \cdot x^2 + 0.0077 \cdot x + 29.2204$. C) ECU force–angle relation obtained by dividing the moment by the moment arm. (D) ECU force-excursion curve. Quadratic fit $y = -0.0525 \cdot x^2 - 0.6765 \cdot x + 28.9814$. The reference length of the ECU is the length at the neutral position, and excursions are the change in tendon path length from the length at neutral.

Currently the outcome of tendon transfer surgeries is not well quantified, and it is felt that with tendon transfer procedures one grade of muscle strength is lost [Friden et al. 1998]. The outcome of the surgery depends on factors such as muscle strength, muscle architecture, tendon moment arm and the joint kinematics [Zajac 1992, Gonzalez et al. 1997]. These factors must be considered when planning a tendon transfer surgery.

In this research we simulate ECU to ECRB tendon transfer surgery using experimental data that can be obtained from individual subjects prior to surgery. The biomechanical simulation assumes that the transferred muscle retains it's length-tension properties, but acts through the moment arm of the target tendon. Thus, to model the tendon transfer procedure one needs to characterize the length-tension properties of the donor muscle and the moment arm of the target tendon. Moments at the wrist joint are measured while stimulating the ECU and the moment arms of the ECU and ECRB are estimated *in vivo* from MRI data. The ECU force-excursion property is computed from the ECU moment and moment arm measurements, and the post-transfer ECU moment is calculated from the computed ECU force-excursion property and the ECRB moment arm measurements. The effects of moment and moment arm measurement errors, along with the effects of reattaching the muscle at different lengths during surgery are examined.

Methods

The wrist moment during surface stimulation of ECU was measured using the wrist moment transducer as described in previous progress reports. The measurements were made with the wrist at different radial and ulnar deviation angles. The stimulation level was fixed at the maximal level for the candidate that did not result in excitation of adjacent muscles. The moment data were fit with a quadratic to obtain the wrist moment as a function of radial-ulnar deviation (Figure 1.a.i.1A).

During tendon transfer surgery the ECU tendon is sutured to the ECRB tendon. Therefore the ECU excursion after transfer is assumed to be equal to, and determined by, the ECRB excursion. The ECRB excursion from the neutral reference position and the ECRB tendon moment arm are estimated from the MR images over a range of flexion-extension angles (Figure 1.a.i.2B). The curve in Figure 1.a.i.2A is the same quadratic as shown in Figure 1.a.i.2D, since the force excursion properties of the ECU are assumed to be the same. However, the individual points superimposed on the curve are the excursions corresponding to the angles at which the ECRB moment arms were estimated. Although the angular range in flexion/extension was similar to the range in radial/ulnar deviation, the excursion covers a smaller portion of the ECU force-excursion curve since the ECRB moment arm in flexion/extension is smaller than the ECU radial/ulnar moment arm *in-situ*. The ECU moment after tendon transfer surgery is calculated as the product of the ECU force and the ECRB moment arm (Figure 1.a.i.2C).

The wrist is assumed to be held in neutral flexion/extension and neutral radial/ulnar deviation during surgery. For the nominal case, the length of the ECU at neutral is not changed by the surgical procedure. In other cases simulations are repeated with the ECU set at different lengths to represent stretching or shortening (tensioning) of the ECU muscle during surgery. A sensitivity analysis of measurement errors on the predicted outcome of the surgery is done.

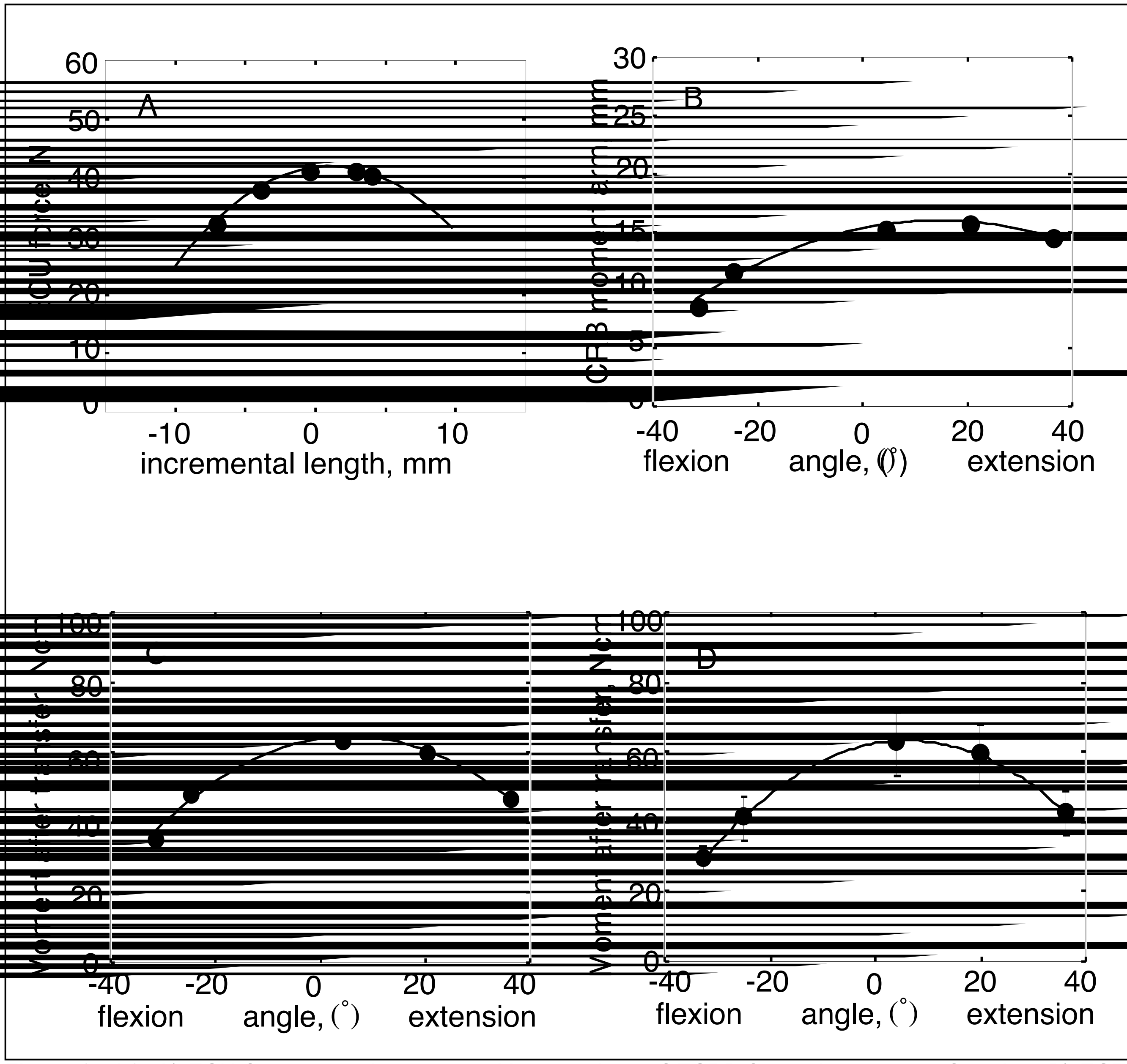

Figure 1.a.i.2. A) ECU force-excursion curve, with excursions of ECRB for a given range of motion. B) ECRB moment arm as a function of flexion-extension angle. C) Moment after transfer due to ECU stimulation as function of flexion-extension angle. Quadratic fit $y = -0.0088 \cdot x^2 + 0.1118 \cdot x + 45.1354$. D) Average moment vs. angle for 1000 simulations with random moment and moment arm errors introduced. The error bars are +/- two standard deviations. Note that the curves in C and D differ because of nonlinearities in the model (even though the mean data source error is zero, the mean effect on the output is nonzero).

Results

The wrist of the same subject was imaged using Magnetic Resonance Imaging to non-invasively estimate the tendon moment arms of the ECU and the ECRB. ECU excursion from a reference position (wrist neutral) and ECU tendon moment arm as a function of radial-ulnar wrist angle are obtained (Figure 1.a.i.1B). At the wrist positions where the ECU moment arms are estimated, the moment calculated from the quadratic equation is divided by the estimated moment arm value to give the ECU force (Figure 1.a.i.1C). The ECU force at the different radial-ulnar angles is plotted as a function of the excursion for that wrist angle (Figure 1.a.i.1D). Another quadratic fit characterizes the force-excursion properties of ECU.

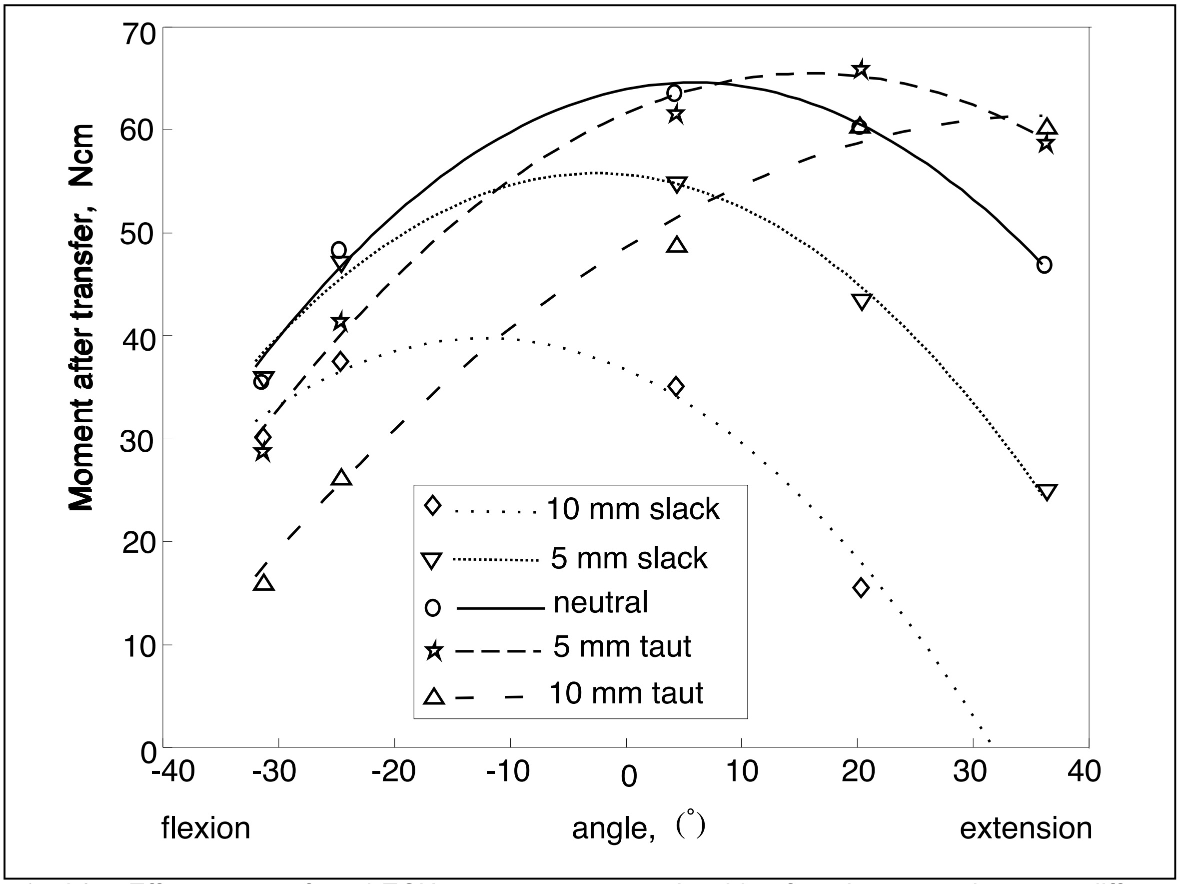

Figure 1.a.i.3. Effect on transferred ECU moment-angle relationship of tendon reattachment at different muscle lengths. The nominal case is when the ECU does not change length as a result of transfer, when measured with the wrist is in the neutral position.

Figure 1.a.i.2C shows the moments predicted after surgery over a range of wrist flexion/extension angles for the nominal case, i.e. no shortening or lengthening of the ECU. The moment at the wrist after transfer varies by approximately 30% over the range shown with a peak at about 10º extension. The shape is similar to the shape of the ECRB moment arm.

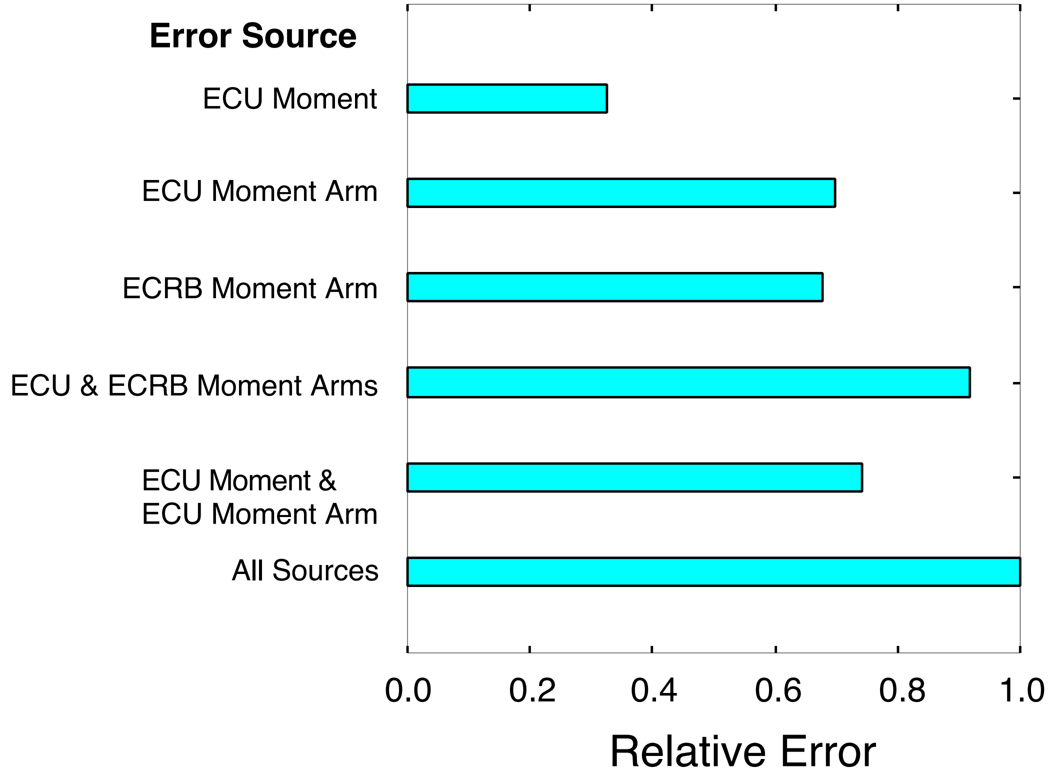

Figure 1.a.i.4. Relative contributions of measurement errors in joint moment and moment arms. The error introduced by different sources and combinations of sources is plotted relative to the error resulting from all sources.

The location of the peak, and the magnitude of the moment are affected by the reattachment length of the ECU (Figure 1.a.i.3). The maximum moment is produced with the ECU set at the length at neutral. Setting the ECU slack moves the ECU to the ascending limb of it's force-excursion curve and the moments decrease at extended angles. At 30° extension the moment decreases from approximately 55 Ncm to 35 Ncm for a 5 mm decrease in ECU length. When the ECU is lengthened it starts to move to the descending limb of it's force-excursion curve and the moments produced at flexed angles decrease. A 6 Ncm decrease for 5 mm lengthening from neutral, and a decrease of 20 Ncm from 38 Ncm to 18 Ncm for a 10mm increase in length are seen at 30° wrist flexion.

Sensitivity analysis was carried out for two reasons, first to establish a range for the predicted values, and second to learn which measurement errors had the greatest effect on the moment predictions. Normally distributed random errors were introduced in the measured moments and moment arms and the variations of the predicted moments were observed. The transducer can have up to 5.5% variance in moment measurements. The moment arm estimates have a repeatability within 10%, except one case with a variation of 25% [Wilson et al. 1999]. The error analysis is done with the worst case variation of 25%. Figure 1.a.i.2D shows the mean moment predicted after transfer for 1000 simulations with random errors. The error bars indicate two standard deviations. The coefficient of variation over the whole set of simulations is 15%. A bootstrap analysis reveals the relative errors introduced by different sources (Figure 1.a.i.4). The maximum error is observed when both moment and moment arm errors are introduced. Relative to this combined error, errors in ECU moment measured before surgery has the smallest effect, while moment arm measurements of either or both muscles contribute quite significantly to the total error.

Discussion

The simulations quantify the wrist extension moments that would be expected after tendon transfer surgery for an individual, based on measurements of his/her own muscle strength and moment arms. These predicted outcomes provide quantitative predictions of surgical outcome, as well as a method of optimizing the outcome for each individual.

The ECU after transfer uses only a part of the force-excursion curve used before surgery, for a similar range of motion. This is because the ECRB moment arm in flexion-extension is smaller then the moment arm of the ECU in radial-ulnar deviation. The smaller moment arm also results in lower moments being produced at the wrist in flexion-extension. The part of the curve used depends on the ECU length at the time of transfer. The ECU length is a function of the wrist position and the reattachment length set by the surgeon.

With the wrist in the neutral position the ECU acts near the plateau of the force-excursion curve. Transferring the ECU at slightly longer lengths decreases the extension moments at flexed positions and increases the individual's ability to achieve wrist extension. Performing the surgery at another wrist position as opposed to neutral changes the reference length of the ECU and thus the part of the force excursion curve used. Because of the importance of muscle reattachment length in determining post-transfer strength, it might be helpful to establish procedures to monitor and control muscle length and wrist position during the transfer procedures. Note in figure 3, reattaching the ECU at the same length as at neutral produces sufficient extension moments to overcome the average net flexion moments at the wrist.

Errors in the estimate of the tendon moment arms have the largest effect on the moment predicted after transfer. It is therefore important to have a high degree of accuracy in the estimation of the moment arms.

It is important to validate this method in future research. One step in the validation would be to compare intra-operative measures of tendon excursion with those estimated from the MRI data. A further step would be to compare intra-operative measures of ECU force-excursion properties with those predicted by the model. Finally, experimentally measured moment-angle curves of the transferred ECU could be compared with the model prediction.

Plans for next quarter

We are working to complete manuscripts describing the wrist moment transducer, as well as our moment arm measurements and tendon transfer simulations.

References

Freehafer A, Kelly C, Peckham P. Planning tendon transfers in tetraplegia: "Cleveland technique", in Tendon Surgery in the hand ed Hunter J, Schneider L, Mackin E. The C. V. Mosby Co., St Louis 1987; chapter 64:506-515.

Friden J, Lieber R. Evidence for muscle attachment at relatively long lengths in tendon transfer surgery. J Hand Surg 1998;23A:105-110.

Fukunaga T, Kawakami Y, Kuno S, Funato K, Fukashiro S. Muscle architecture and functions in humans. J Biomech 1997;30:457-463.

Gonzalez R, Buchanan T, Delp S. How muscle architecture and moment arms affect wrist flexion-extension moments. J Biomech 1997;30:705-712.

Keith M, Kilgore K, Peckham P, Wuolle K, Creasey G, Lemay M. Tendon transfers and functional electrical stimulation for restoration of hand function in spinal cord injury. J Hand Surg 1996;21:89-99.
Keith M. Restoration of tetraplegic hand function using an FES neuroprosthesis, in Tendon and nerve surgery in the hand a third decade ed Hunter J, Schneider L, Mackin E. Mosby St. Louis 1997; chapter 28:226-231.
Lieber R, Friden J. Intraoperative measurement and biomechanical modeling of the flexor carpi ulnaris-to-extensor carpi radialis longus tendon transfer. J Biomed Eng. 1997;119:386-391.
Lieber R, Friden J. Musculoskeletal balance of the human wrist elucidated using intraoperative laser diffraction. J Electromyogr & Kinesiol 1998;8:93-100.
Loren G, Shoemaker S, Burkholder T, Jacobson M, Friden J, Lieber R. Human wrist motors: biomechanical design and application to tendon transfers. J Biomech 1996;29:331-342.
Pedretti, L.W.; Zoltan, B.; "Occupational Therapy practice skills for physical dysfunction," **3rd** edition, The C. V. Mosby Company, St. Louis, 1990.
Pigeon P, Yahia H, Feldman A. Moment arms and length of human upper limb muscles as functions of joint angles. J Biomech 1996;29:1365-1370.
Zajac F. How musculotendon architecture and joint geometry affect the capacity of muscles to move and exert force on objects: A review with application to arm and forearm tendon transfer design. J Hang Surg. 1992;17:799-804.

1.a.ii. PASSIVE AND ACTIVE MOMENTS

Abstract

Previously, we reported that the position of the metacarpal phalangeal (MP) joint of the long finger had a strong influence on the passive properties recorded for the MP joint of the index finger. We verified that the angle of the long finger MP joint has a significant effect on the passive properties of the index finger MP joint over the whole range of long finger positions. During this quarter we have worked on modifications to our measurement apparatus in order to obtain additional information regarding this effect.

Purpose

The purpose of this project is to characterize the passive properties of normal and paralyzed hands. This information will be used to determine methods of improving hand grasp and hand posture in FES systems.

Progress Report

During the previous quarter, we worked on developing simple splints that will allow us to position the PIP joint at three different joint angles (0,45 and 90º). During this quarter we have worked on further modifications to the apparatus and software to make the apparatus more robust and stable, easier to setup and adjust and allow us to operate on Windows platform, rather than Macintosh. The side supports were reinforced to prevent side to side movements on the measurement beam. A follower gear was added to reduce the backlash of the drive chain. The measurement amplifiers were incorporated into the enclosure with the torque motor controls. Provision was made to control the limit switches by both mechanical (hitting the switch) and logical control (software, based on torque limits). The data acquisition routines written in Labview were transferred to Windows based Labview 5.0 and are in the process of being revised to incorporate software control of torque limits.

Plans for Next Quarter

During the next quarter, we will perform experiments to examine the effect of adjacent digit position on passive properties. These experiments will focus on the effect of the PIP joint position.

1. b. BIOMECHANICAL MODELING: ANALYSIS AND IMPROVEMENT OF GRASP OUTPUT

Abstract

Previous model simulations indicate that surgical tensioning of the Br-ECRB tendon transfer influences both active wrist extension and gravity-assisted wrist flexion. Simulations also indicate that wrist function is dependent on elbow position after transfer. A preliminary analysis of clinical data indicates that wrist function can vary substantially across subjects after a Br-ECRB tendon transfer, and that the active range of motion at the wrist could be improved in each of the seven subjects studied. Elbow dependent wrist function was identified in five of seven subjects studied. Preliminary model simulations indicate that moving the origin of the brachioradialis distally on the humerus could have wrist function could be improved after Br-ECRB tendon transfer.

Objective

The purpose of this project is to use the biomechanical model and the parameters measured for individual neuroprosthesis users to analyze and refine their neuroprosthetic grasp patterns.

In the past quarter, we have evaluated how the passive moment-generating capacity of the tight and slack Br-ECRB transfer (described in previous progress reports) influences gravity-assisted wrist flexion. The net passive moment at the wrist joint (before a Br-ECRB transfer) was compared to the passive wrist extension moment generated by the transfer to estimate the range of wrist postures where gravity-assisted wrist flexion is possible.

Progress Report

In the past quarter, we have continued to evaluate patient data from our clinical research laboratory to assess wrist function after the Br-ECRB tendon transfer. In particular, we are focusing on the link between wrist function and elbow position. Model simulations have been expanded to evaluate how wrist function would be affected if the origin of the brachioradialis was moved distally on the humerus. In addition, Wendy Murray traveled to the ASME 1999 Bioengineering Conference in Bozeman, Montana and gave a podium presentation entitled "Surgical Simulation of the Br-ECRB Tendon Transfer." The two page abstract is included with this progress report.

<u>Evaluating the Br-ECRB tendon transfer in patients</u>

A follow-up of Br-ECRB tendon transfer patients is being carried out in our clinical laboratory. In the previous progress report, we summarized the difference between the passive range of motion at the wrist before and after a Br-ECRB tendon transfer in nine individuals. At this point, we have identified sixteen individuals with Br-ECRB tendon transfers who are candidates for further study. In seven of those sixteen, we have tested the wrist extension position that can be maintained against gravity in three different elbow positions. In these seven subjects, the maximum wrist extension position ranged between 27° and 55°. Wrist extension varied as a function of elbow position in five individuals; four of these five individuals lost wrist extension as the elbow was flexed (Fig. I.b.1). The passive range of wrist extension was less dependent on elbow position (Fig. I.b.2).

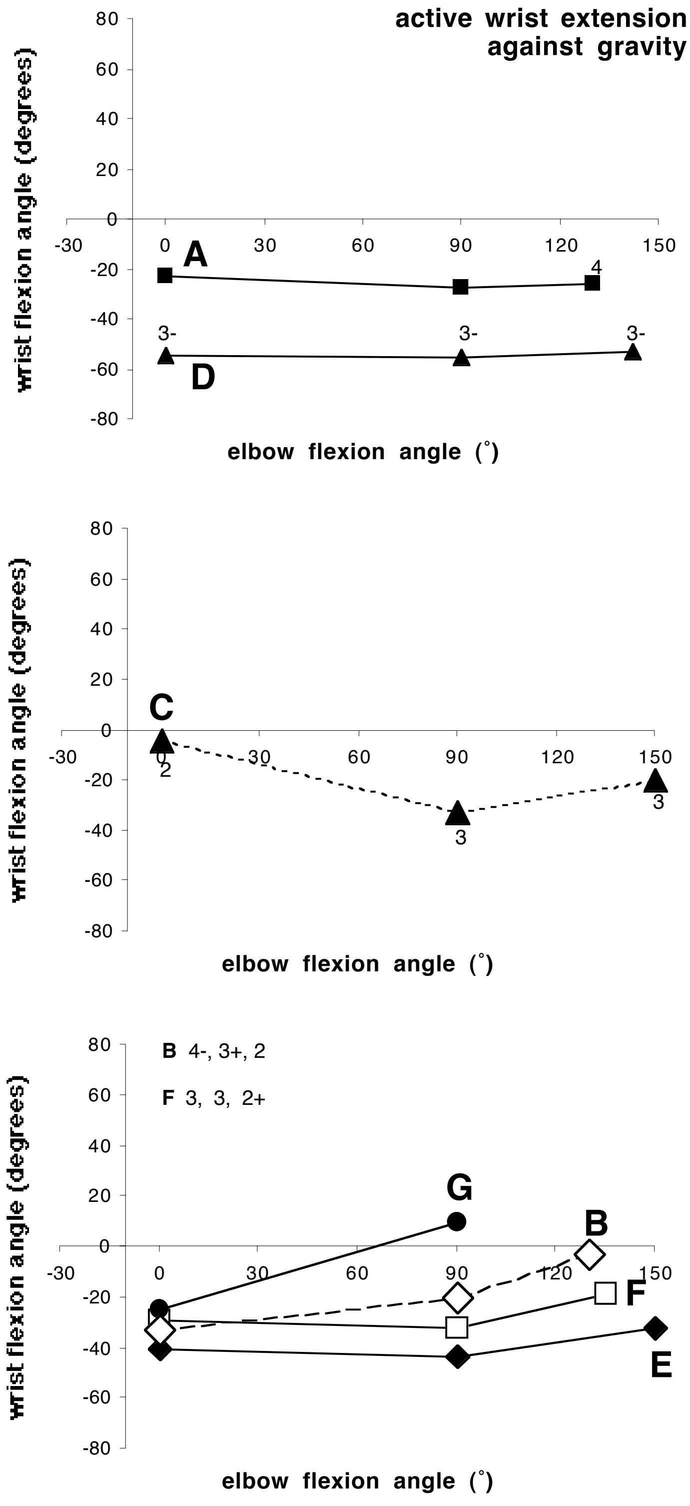

Figure I.b.1. Wrist extension position actively generated against gravity by seven individuals with Br-ECRB tendon transfers. Positive numbers indicate wrist flexion; negative numbers indicate wrist extension. 0˚ elbow flexion is full extension. Subjects A and D were able to maintain a consistent wrist position over a broad range of elbow postures. Subject C had less wrist extension when the elbow was extended compared to when the elbow was flexed. Subjects B, E, F, and G lost wrist extension as the elbow was flexed. Manual muscle grades are indicated for the subjects and arm positions where available.

The rest position of the wrist was measured at different elbow positions in four of the seven subjects (Fig. I.b.3). The rest position of the wrist was in flexion in each subject, the maximum flexion position ranged from 17˚ flexion in Subject A to 74˚ flexion in Subject B. Rest wrist position showed a strong dependence on elbow posture in Subject B, increasing from 34˚ flexion at 0˚ elbow extension to 74˚ flexion at 130˚ flexion. The large change in rest wrist position with elbow flexion implies the passive properties at the wrist joint vary with elbow position in Subject B. Based on this data, we hypothesize that the passive extension moment was substantially greater at full elbow extension than full flexion. Notably, active wrist extension is minimal for Subject B in full elbow flexion. The dependence of both active wrist extension and rest wrist position on elbow posture in Subject B correlates well with model predictions of how wrist function changes with wrist posture given a slack tendon transfer.

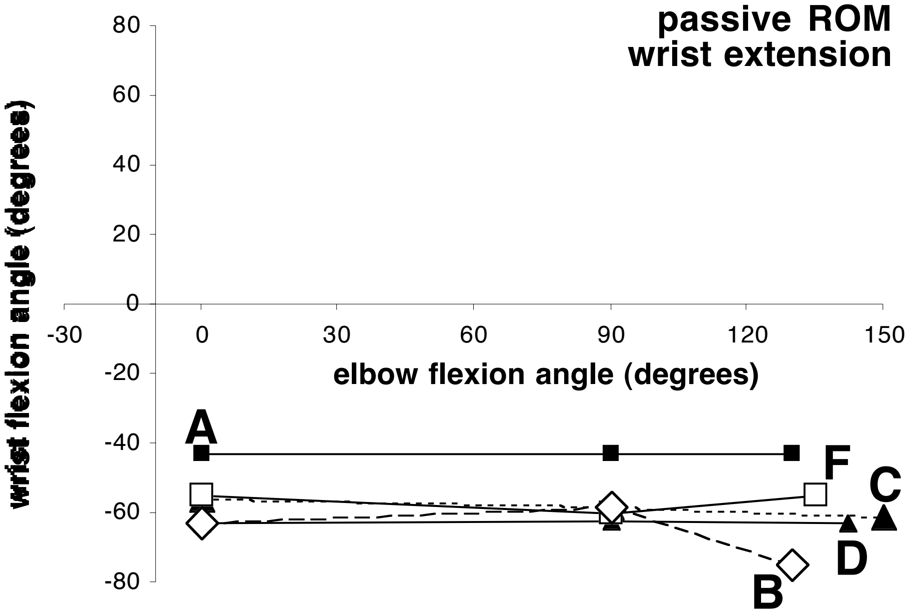

Figure I.b.2. Passive range of motion for wrist extension, measured in five individuals with Br-ECRB tendon transfers. Positive numbers indicate wrist flexion; negative numbers indicate wrist extension. 0˚ elbow flexion is full extension. The passive range of wrist extension is less dependent on elbow posture than the active range of motion (cf. Figure 1).

At 90˚ elbow flexion, active wrist extension against gravity did not reach the limit of passive extension in any of the seven individuals studied, indicating the active range of motion at the wrist could be improved in all subjects (Figure I.b.4). The rest wrist position reached the limit of passive flexion in one subject only (Subject F).

Simulation of Distal Transfer of the Origin of the Brachioradialis

The brachioradialis has the largest elbow flexion moment arm of any of the muscles that cross the elbow (Murray, *et al.*, 1995), which results in a substantial change in length as the elbow moves through its range of motion. Because of this large length change, the brachioradialis operates over a broad portion of the isometric force-length curve during elbow flexion. Previous model simulations of wrist function after the Br-ECRB tendon transfer indicate that this broad operating range can compromise the function of the brachioradialis after transfer to the ECRB. If the surgeon performs a slack transfer, muscle fibers may become too short to generate adequate active force to maintain an extended wrist when the elbow is fully flexed. If the surgeon performs a tight transfer, muscle fibers reach long enough lengths to generate a substantial amount of passive force, limiting passive wrist flexion when the elbow is extended. Moving the origin of the brachioradialis distally on the humerus would move the muscle path closer to the axis of elbow flexion, reducing the elbow flexion moment arm and the length change the muscle experiences during elbow rotation. Distal transfer of the origin would also reduce the elbow flexion moment generated by the brachioradialis.

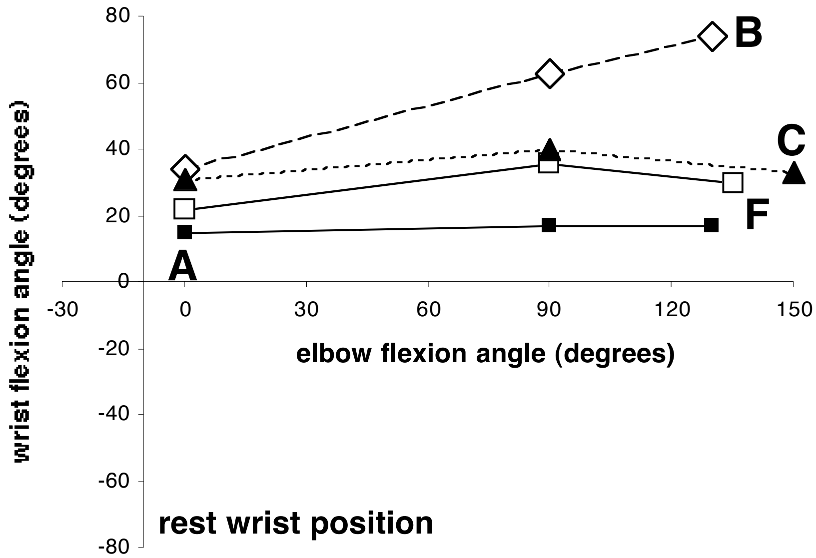

Figure I.b.3. Rest wrist position, as a function of elbow position, measured in four individuals with Br-ECRB tendon transfers. Positive numbers indicate wrist flexion; negative numbers indicate wrist extension. 0˚ elbow flexion is full extension. Rest wrist position was in flexion in each subject, and was highly dependent on elbow position in Subject B.

In the past quarter, we developed a computer simulation of distal transfer of the origin of the brachioradialis. The new origin was incorporated into the modeled muscle path of the Br-ECRB tendon transfer. The goal of this work is to evaluate how moving the origin of the brachioradialis would influence wrist function after Br-ECRB tendon transfer. The force-generating properties of the Br-ECRB tendon transfer differ when the origin is moved. First, because the elbow flexion moment arm of the brachioradialis is reduced, the muscle fibers use less of the isometric force-length curve. In addition, the fiber length vs. elbow flexion angle relationship can be altered. For example, if the surgeon first sets the relationship between muscle fiber length and joint angle (i.e., tensions the transfer), and then moves the origin of the brachioradialis, moving the origin would serve to make both a tight and a slack transfer *more slack* than the surgeon originally set. That is, after moving the origin, either a slack or a tight transfer would operate at shorter fiber lengths than originally tensioned.

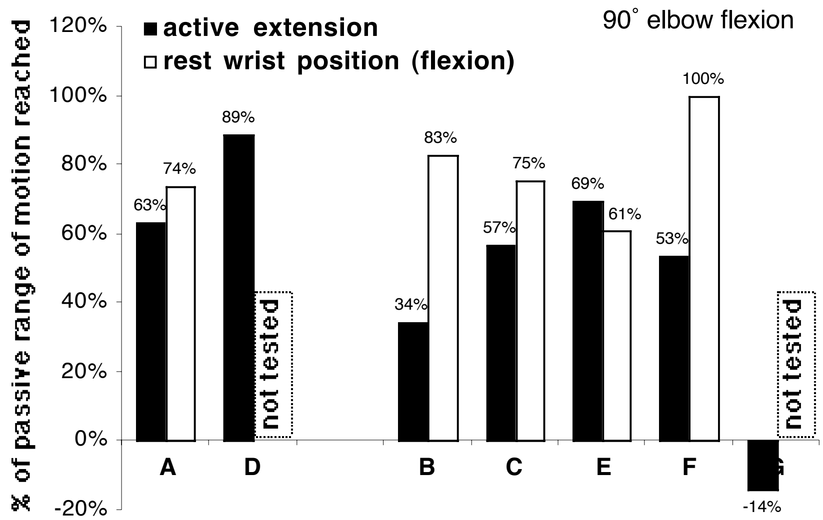

Figure I.b.4. Active wrist extension position and rest wrist position at 90˚ elbow flexion expressed as a percentage of the total passive range of motion in wrist extension and flexion, respectively. Active wrist extension did not reach the limits of passive extension in any of the seven subjects. Rest wrist position reached the limit of passive wrist flexion only in Subject F. Rest wrist position was not tested in subjects D and G. Subjects A and D are the two subjects where wrist extension did not change with elbow position. These results indicate that the active range of motion at the wrist could be increased in all subjects.

We have completed a simulation of wrist function after distal transfer of the origin, using the paradigm that the surgeon first tensions the transfer and then moves the origin. Wrist function predicted by the previously described models of the Br-ECRB slack and tight transfers was compared to wrist function after distal transfer of the brachioradialis origin to three different sites: distal transfer by 1 cm (❒ 1 cm), 2 cm (❒ 2 cm), and 3 cm (❒ 3 cm). Table I.b.I shows the peak moment arms and musculotendon lengths of the Br-ECRB transfer with and without distal transfer of the origin.

TABLE I.b.I.

PEAK MOMENT ARM AND MUSCULOTENDON LENGTH OF BR-ECRB TRANSFER WITH AND WITHOUT DISTAL TRANSFER OF THE ORIGIN OF BRACHIORADIALIS*

	PEAK MOMENT ARM	MUSCULOTENDON LENGTH (0˚ ELBOW FLEXION)	MUSCULOTENDON LENGTH (90˚ ELBOW FLEXION)
Br-ECRB	8.8	38.3	31.8
❒ 1 cm	7.9	37.4	31.4
❒ 2 cm	7.0	36.6	31.0
❒ 3 cm	6.1	30.8	30.8

** data in cm*

If the origin of the brachioradialis is moved after a tight Br-ECRB tendon transfer has been performed (tendon slack length = 0.14 m), the wrist extension moment generated as a function of elbow flexion angle is similar to the tight transfer without the distal transfer (Fig. I.b.5A). All three distal transfer sites result in a Br-ECRB transfer that has sufficient moment-generating capacity to maintain 40˚ wrist extension between 0˚ and 130˚ elbow flexion. The passive moment generated at the wrist changes if the origin is moved, influencing the range of gravity-assisted wrist flexion (Fig. I.b.5B). The rest position of the wrist at full elbow extension shifts toward more flexed postures as the origin is moved distally on the humerus. If a tight transfer is performed and the origin is not moved, the equilibrium position of the wrist predicted by the model is 18˚ wrist extension. When the origin is moved distally by 1 cm, the rest wrist position shifts to 6˚ wrist extension. Moving the origin by 2 cm shifts the equilibrium position to 4˚ wrist flexion, while a transfer of 3 cm shifts the rest position to 10˚ wrist flexion. The equilibrium position of the wrist for a slack transfer (without moving the origin) is 12˚ wrist flexion. Thus, performing a tight transfer and then moving the origin of the brachioradialis yields a Br-ECRB transfer that produces adequate wrist extension over a broad range of elbow postures, but provides more passive wrist flexion than the original tight transfer. If the origin is moved after a slack transfer (tendon slack length = 0.17 m), gravity-assisted flexion improves further, with rest wrist positions of 18˚ wrist flexion, 22˚ wrist flexion, and 24˚ wrist flexion for 1 cm, 2 cm, and 3 cm origin transfers. However, like the conventional slack transfer, the wrist extension moment decreases substantially with elbow flexion, and the slack transfer cannot provide 40˚ wrist extension in flexed elbow postures, even if the origin is moved.

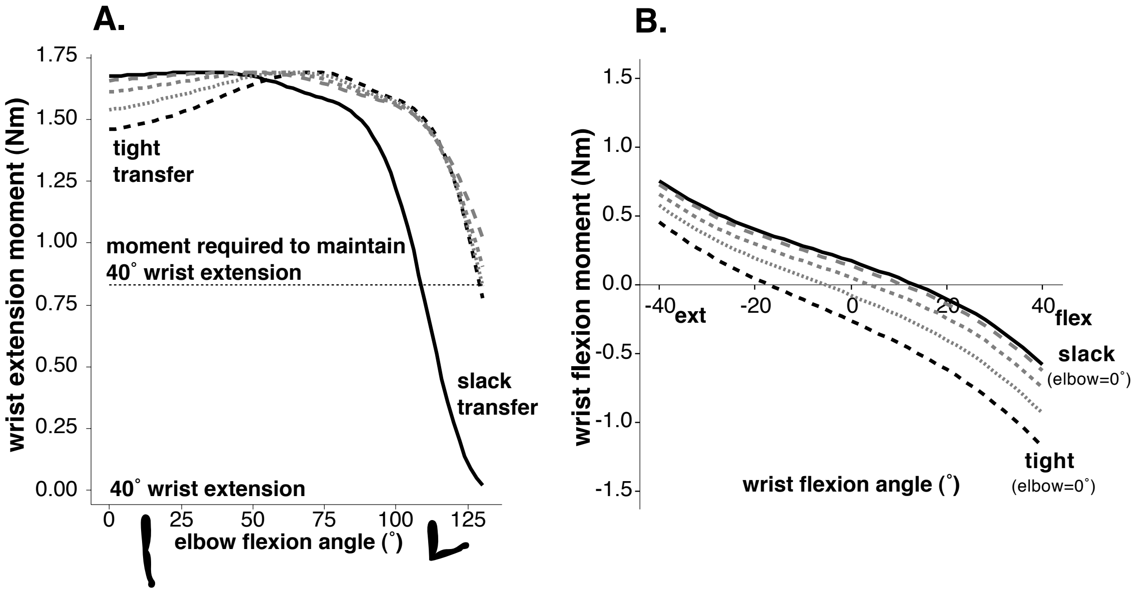

Figure I.b.5. (A) Wrist extension moment generated by the slack transfer (solid black line), tight transfer (dashed black line), and tight transfer with origin moved distally by 1 cm, 2 cm, and 3 cm (dashed gray lines) as a function of elbow position. (B) Passive wrist flexion moment generated when the elbow is fully extended by the slack transfer (solid black line), tight transfer (dashed black line), and tight transfer with origin moved distally by 1 cm, 2 cm, and 3 cm (dashed gray lines) as a function of wrist position. If the origin of the brachioradialis is moved distally on the humerus after a tight transfer, the Br-ECRB transfer can provide adequate wrist extension moment to maintain 40˚ wrist extension between 0˚ and 130˚ elbow flexion. In addition, the rest wrist position is in a more flexed posture than if a tight transfer is performed and the origin is not moved.

Moving the origin of the brachioradialis distally on the humerus also has risks. The brachioradialis originates from the supracondylar ridge of the humerus, and is a fibrous, broad origin. In the cadavers specimen on which the upper extremity model is based, the origin of the brachioradialis covered approximately 8 cm of the length of the bone. Moving the origin of the brachioradialis would be a challenging surgical technique, and requires an anatomical investigation to determine if the blood and nerve supplies could withstand the move. If moving the origin caused ischemia of the muscle, damaged the nerve supply, or resulted in a loss of muscle force-generating capacity via other means, wrist function after transfer could be severely compromised (Fig. I.b.6). Both the potential risks and potential benefits of moving the brachioradialis origin need to be further considered.

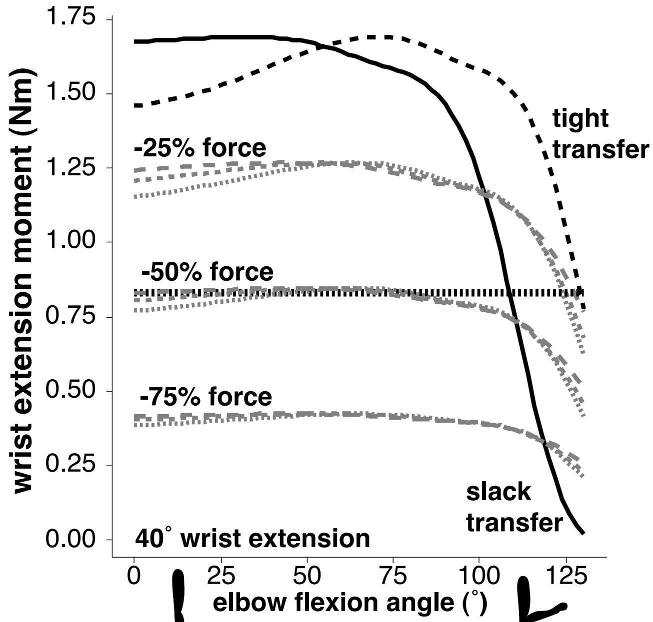

Figure I.b.6. Wrist extension moment generated by the slack transfer (solid black line), the tight transfer (dashed black line), and the tight transfer with origin moved distally, assuming a 25%, 50%, and 75% decrease in force-generating capacity of the muscle post-operatively (groups of dashed gray lines). If moving the origin were to cause ischemia of the muscle, damage the nerve supply, or result in a loss of muscle force-generating capacity via other means, wrist function after transfer could be severely compromised. It is important to further evaluate the surgical risks involved with distal transfer of the origin of the brachioradialis.

Plans for Next Quarter

In the next quarter, we plan to continue the evaluation of wrist function after distal transfer of the brachioradialis origin. We plan to simulate the effects of tensioning the transfer after moving the origin, which would alter the relationship between fiber length and elbow flexion angle from the model discussed in this progress report. Also, we will investigate the effect of moving the origin on the elbow flexion moment generated by the brachioradialis. In addition, we are planning an investigation of the anatomical and surgical issues involved in this procedure. Dr. Michael Keith and an orthopaedic surgical resident will be involved in this aspect of the study. Also in the next quarter, we will continue evaluation of wrist function in individuals with a Br-ECRB transfer. Now that we have identified differences in wrist function across subjects, we will begin contacting individuals and collecting quantitative strength measurements using the elbow and wrist moment transducers.

References

Murray, W. M., Delp, S. L. and Buchanan, T. S. (1995) Variation of muscle moment arms with elbow and forearm position. *J Biomechanics* **28,** 513-525.

2. CONTROL OF UPPER EXTREMITY FUNCTION

Our goal in the five projects in this section is to either assess the utility of or test the feasibility of enhancements to the control strategies and algorithms used presently in the CWRU hand neuroprosthesis. Specifically, we will: (1) determine whether a portable system providing sensory feedback and closed-loop control, albeit with awkward sensors, is viable and beneficial outside of the laboratory, (2) determine whether sensory feedback of grasp force or finger span benefits performance in the presence of natural visual cues, (of particular interest will be the ability of subjects to control their grasp output in the presence of trial-to-trial variations normally associated with grasping objects, and in the presence of longer-term variations such as fatigue), (3) demonstrate the viability and utility of improved command-control algorithms designed to take advantage of forthcoming availability of afferent, cortical or electromyographic signals, (4) demonstrate the feasibility of bimanual neuroprostheses, and (5) integrate the control of wrist position with hand grasp.

2. a. HOME EVALUATION OF CLOSED-LOOP CONTROL AND SENSORY FEEDBACK

Abstract

The purpose of this project is to deploy an existing portable hand grasp neuroprosthesis capable of providing closed-loop control and sensory feedback outside of the laboratory. We have completed the development of a stand alone, analog, single channel stimulator for grasp-force feedback. The field tests for of the prototype unit described in the prior report were delayed and will be pursued in the forthcoming quarter.

Purpose

The purpose of this project is to deploy a portable hand grasp neuroprosthesis capable of providing closed-loop control and sensory feedback outside of the laboratory. Our goal is to evaluate whether the additional functions provided by this system benefit hand grasp outside of the laboratory.

Progress Report

No progress to report this quarter.

Plans for Next Quarter

As originally planned for the previous quarter, we will make a set of short-run (1 day) field tests of the α-prototype on neuroprosthesis users in order to detect and correct remaining design problems. We are particularly concerned about the ergonomics of the sensor and electrode. Pending successful completion of the tests, we will produce 5-6 units for field deployment.

2. b. INNOVATIVE METHODS OF CONTROL AND SENSORY FEEDBACK

2. b. i. ASSESSMENT OF SENSORY FEEDBACK IN THE PRESENCE OF VISION

Abstract

The purpose of this project is to develop a method for including realistic visual information while presenting grasp-force feedback information simultaneously, and to assess the impact of force feedback on grasp performance in the presence of such visual information. In this quarter, we completed the initial project evaluating the effects of grasp force feedback in the presence of vision and have submitted a manuscript to Medical and Biological Engineering and Computing (abstract included below; full text provided confidentially to Program Officer).

Purpose

The purpose of this project is to develop a method for including realistic visual information while presenting other feedback information simultaneously, and to assess the impact of feedback on grasp performance. Vision may supply enough sensory information to obviate the need for supplemental proprioceptive information via electrocutaneous stimulation. Therefore, it is essential to quantify the relative contributions of both sources of information.

Progress Report

The primary accomplishment this quarter was the completion of the initial study and a manuscript entitled “Effectiveness of supplemental grasp-force feedback in the presence of vision,” which was submitted to Medical & Biological Engineering & Computing. The abstract is included below, and a full-text copy of the manuscript has been sent to the Program Officer.

Abstract

“Many previous studies have shown that supplemental, grasp-force feedback can improve grasp control for users of a prosthesis or neuroprosthesis under conditions where vision provides little information about grasp force. Visual cues of force are widely available in everyday use, however, and may obviate the utility of other, supplemental force information. The purpose of the present study was to use a video-based, hand neuroprosthesis simulator to determine whether grasp-force feedback can improve grasp control in the presence of realistic visual information. Seven able-bodied subjects used the simulator to complete repetitions of a simple grasp-and-hold task while controlling and viewing pre-recorded, digitized, video clips of a neuroprosthesis user’s hand squeezing a compliant object. The task was performed with and without supplemental force feedback presented via electrocutaneous stimulation. In the task, subjects had to achieve and maintain the (simulated) grasp force within a target window of variable size. Force feedback improved the success rate equally and significantly for all target window sizes, on average, and improved the success rate at all window sizes for 6 of the 7 subjects. Overall, the improvement was equivalent functionally to a 35% increase in the window size. Feedback also allowed subjects to identify the direction of grasp errors (forces too high or too low) more accurately. In some cases, feedback improved the failure identification rate even if success rates were unchanged. We conclude, then, that supplemental grasp-force feedback can improve grasp control even with access to rich visual information from the hand and object.”

Plans for Next Quarter

We will also initiate continuing studies on the effects of object and task parameters on the relative contributions of visual and grasp force feedback.

2. b. ii. INNOVATIVE METHODS OF COMMAND CONTROL

Abstract

The purpose of this project is to develop new command control algorithms that will make control of neural prosthetic hand grasp simpler and more effective. During this quarter the new acquire-hold-modify evaluation task was implemented in the video-based simulation system. Using the new task, testing of the seven different command/control algorithms was conducted. The data indicate that performance using the various algorithms was consistent across sessions within subjects. Further, these data suggest that two new command control algorithms, A new experimental protocol, similar to a response surface design, was developed which detailed the testing procedure to most efficiently compare the algorithms in future testing.

Purpose

The purpose of this project is to improve the function of the upper extremity hand grasp neuroprosthesis by improving user command control. We are specifically interested in designing algorithms that can take advantage of promising developments in (and forthcoming availability of) alternative command signal sources such as EMG, and afferent and cortical recordings. The specific objectives are to identify and evaluate alternative sources of logical command control signals, to develop new hand grasp command control algorithms, to evaluate the performance of new command control sources and algorithms with a computer-based video simulator, and to evaluate neuroprosthesis user performance with the most promising hand grasp controllers and command control sources.

Progress Report

1. New Evaluation Task

The new acquire-hold-modify evaluation task was implemented in the video-based evaluation system. In performing this task, the user first acquires a force within a specific force window by elevating or depressing their shoulder. The subject then locks the command at that level through a rapid elevation of the shoulder, if the algorithm under test requires a lock, or maintains the command within the force window (hold). In the final part of the task, the subject adjusts the output of the hand to fit into a new force window (modify). The widths of the force widows are determined by varying the widow size variable. While both widows are varied by the same percentage, the second window is larger because the force is calculated relative to the target force, and the target force for the second window is higher. However, the second force window is often more difficult to achieve since the force recruitment curve for the simulated hand is steeper in that command range.

2. Testing of Command/Control Algorithms

Preliminary testing of the command/control algorithms was conducted. During each testing session, the subject completed nine experimental blocks. Each block was composed of 15 trials of the evaluation task described above. The blocks were performed in groups of three- one algorithm at three different force window sizes. The first algorithm tested was always the baseline algorithm, which uses only proportional control. The baseline algorithm will be used to normalize the results across subjects and sessions. The remaining two groups of three blocks are used to test two other algorithms. During the preliminary testing, combinations of two pairs of algorithms were tested in multiple sessions with multiple subjects. This gave some insight as to the repeatability of the data.

Using Cochran-Mantel-Haenszel Statistics as a means of comparison, the baseline algorithm data was shown to be consistent across sessions within subjects. This allows the data to be compared by normalizing all data in one session to the baseline in that session. Further analysis showed that all of the algorithms tested during the preliminary testing were consistent across sessions within subjects.

Five different command control algorithms have been tested to date: baseline proportional control, threshold rectified lock, proportional rectified lock, proportional control with lock, and the variable gain algorithm. A state diagram for the threshold rectified lock algorithm and the proportional rectified lock algorithm appeared in an earlier progress report. State diagrams for the lock only algorithm (which is the algorithm currently used in upper-extremity neuroprostheses) and the variable gain algorithm are shown in Figure C.2.b.ii.1.

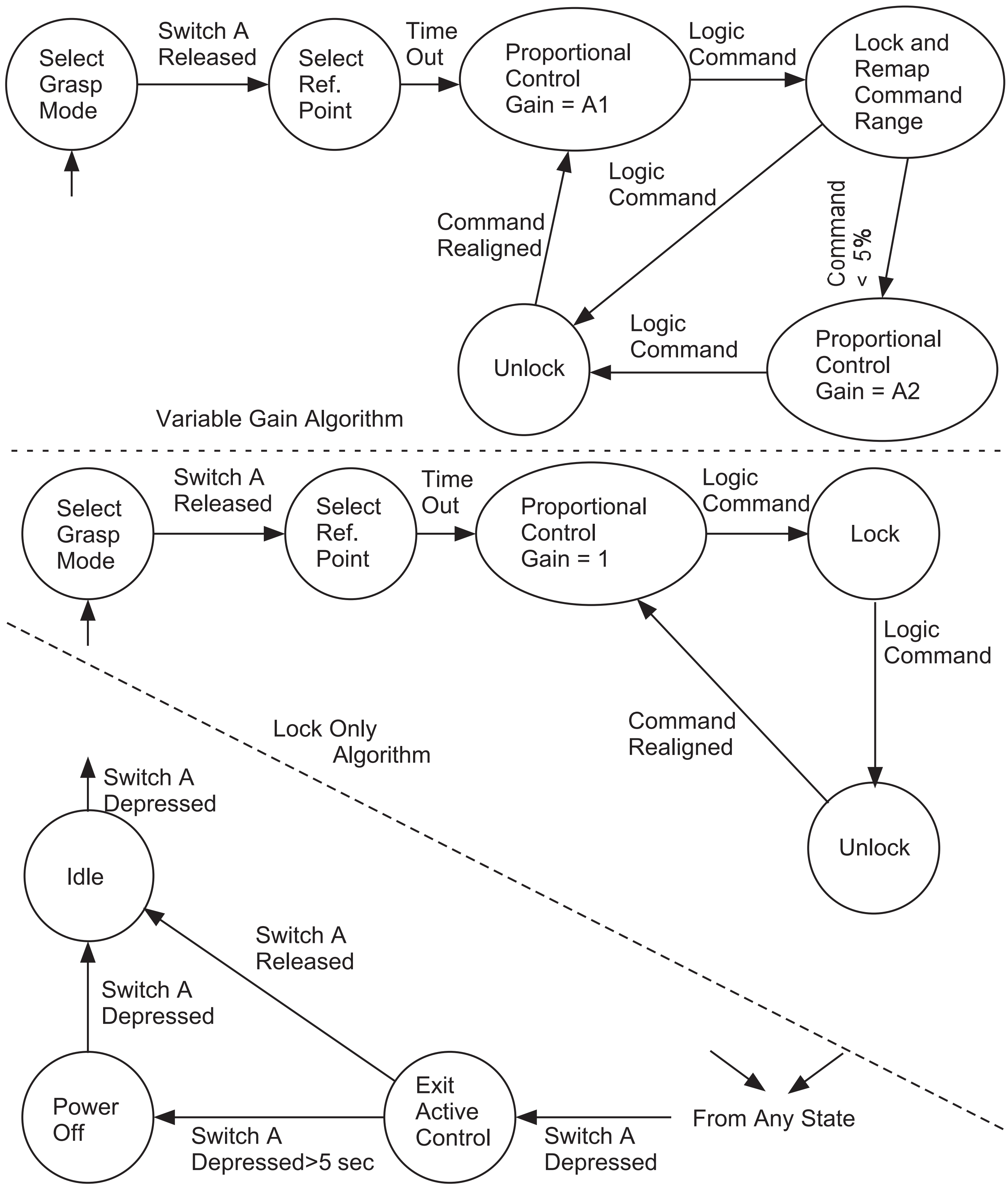

Figure C.2.b.ii.1. State diagrams for lock only algorithm and variable gain algorithm. The diagram under the slanted dashed line is the same for both algorithms.

The percentage success in the acquire-hold-modify task, using different command control algorithms, is plotted in figures C.2.b.ii.2 and C.2.b.ii.3. Each point is the mean success rate over all trials in all sessions for each subject. A generalized linear model was used to compare the performance with each algorithm relative to the baseline algorithm. The model used a binomial error since all of the data was in pass/fail form and a logit link to transform the data from a binomial distribution to a normal distribution. The control variables were the subject, the session number, and the algorithm. The most important result obtained from this model compared the performance of each of the algorithms relative to the baseline algorithm. According to this result, the performance of the variable gain algorithm was significantly better than the baseline algorithm (p=0.0053), and the proportional rectified-lock algorithm was slightly better than the baseline algorithm (p=0.065). The differences between the baseline algorithm and the other algorithms tested in the preliminary testing were statistically insignificant.

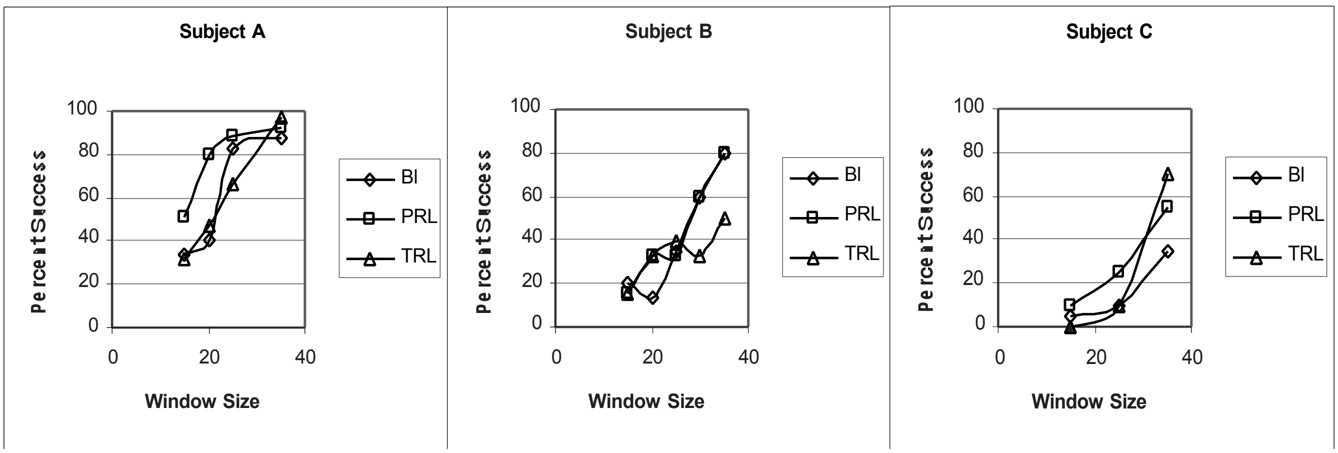

Figure C.2.b.ii.2. Percentage success in the acquire-hold-modify task (mean of all trails in all sessions) for each subject comparing the baseline proportional control algorithm (Bl), the threshold rectified lock algorithm (TRL), and the proportional rectified lock algorithm (PRL).

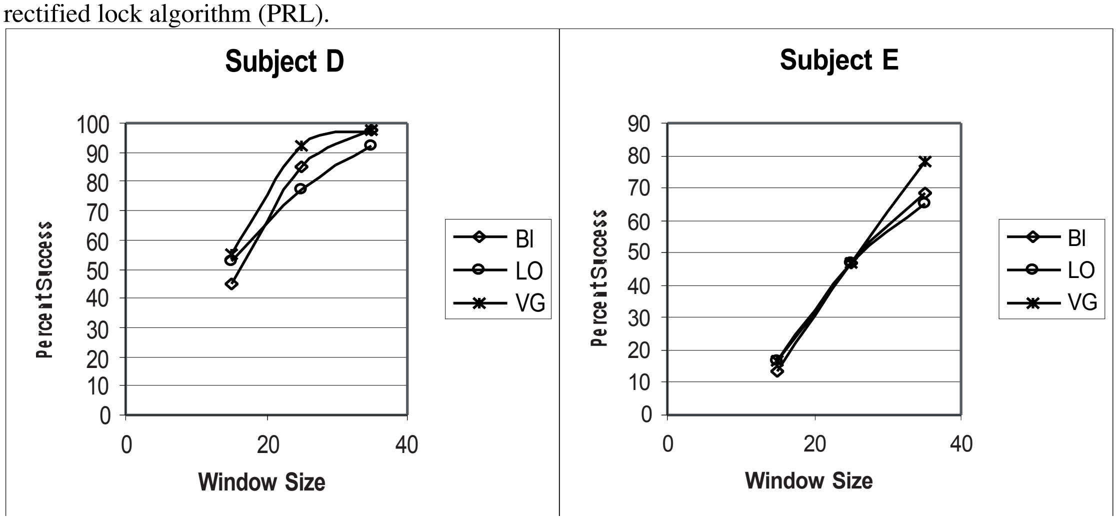

Figure C.2.b.ii.3. Percentage success in the acquire-hold-modify task (mean of all trails in all sessions) for each subject comparing the baseline proportional control algorithm (Bl), the proportional control plus lock algorithm (LO), and the variable gain algorithm (VG).

3. Experimental Design

An experimental design approach, similar to a response surface design, has been developed to minimize the number of sessions needed to compare all command control algorithms,. In following this design, one session will be run for each combination of algorithms. This will enable us to disperse points evenly across the response surface. The entire surface composed of the combinations of the various dimensions can then be examined to see where additional testing is needed to optimize statistical significance. The response surface design is useful because of the large number of categories within each dimension of this experiment.

Plans for Next Quarter

Testing will be continued using the protocol consistent with the new experimental design described above. Effort in the next quarter will focus on the continued evaluation of new command control algorithms using the video simulator.

2. b. iii . INCREASING WORKSPACE AND REPERTOIRE WITH BIMANUAL HAND GRASP

Abstract

Examination of the possible EMG contamination of the frontal beta rhythm was conducted using spectral analysis. Data collected from four subjects while they were deliberately activating the muscles of facial expression (corrigator, frontalis, masseter/temporalis and platysma) was compared to the normal cursor movement condition. Analysis indicated that there was a minimal level of contamination of the signal by muscle activity. However, this was not enough to account for the voltage differences seen during normal cursor movement. Therefore, it has been concluded that the signal is primarily a cortical signal.

Purpose

The objective of this study is to extend the functional capabilities of the person who has sustained spinal cord injury and has tetraplegia at the C5 and C6 level by providing the ability to grasp and release with both hands. As an important functional complement, we will also provide improved finger extension in one or both hands by implantation and stimulation of the intrinsic finger muscles. Bimanual grasp is expected to provide these individuals with the ability to perform over a greater working volume, to perform more tasks more efficiently than they can with a single neuroprosthesis, and to perform tasks they cannot do at all unimanually.

Progress Report

The use of the frontal beta rhythm for the operation of the neuroprosthesis has raised questions concerning the origin of the signal. Since the signal is being recorded from the frontal areas, we have wanted to insure that subjects are not deliberately generating muscle contractions to generate the control signal. Therefore, work in the past quarter has focused on addressing this question.

The brain-computer interface (BCI) was adapted so that the control signal was sampled at a 3 kHz frequency and the low pass filter on the EEG amplifier was adjusted up to 1 kHz. In this manner, it would be possible to record both the EEG (1-45 Hz) and EMG (60 – 1000 Hz) components of the control signal. The subject was then asked to move the cursor as they normally would, or to use muscle relaxation and contraction to move the cursor on the computer screen. The muscles that were activated were the corrugator, the frontalis, the temporalis/masseter, and the platysma. Four of the subjects who have been trained to control the frontal beta rhythm with a high degree of accuracy (> 90%) have participated in the experiment. Analysis of the data consisted of performing a Fast-Fourier Transform (FFT) of the data set between 1 and 500 Hz, and then examining the energy distribution in both the EEG and EMG signal bands.

Figure 2.b.iii.1 shows the spectral plots for the normal cursor movement condition compared to frontalis muscle activation in one subject. The spectra are plotted on a log-log scale to accentuate voltage differences. As can be seen in the figure, the spectra for the muscle demonstrates a much greater energy component in the higher frequencies compared to the normal cursor movement condition. This was true for all of the muscles except for the corrugator, which did not exhibit the high frequency energy peak in two of the subjects. However, given that the recording site for each of these subjects was the F3 electrode and that the corrugator muscle is approximately 6 centimeters away, its activity was not anticipated to be recorded at this site.

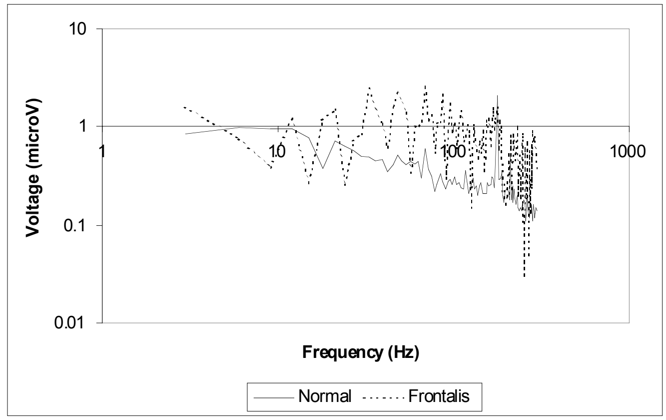

Figure 2.b.iii.1 - Spectral Analysis of EMG and Control Signal

The data collected under the normal cursor movement condition, although not exhibiting the large energy component in the EMG band, did not rule out the possibility of low-level EMG contamination. Therefore, to address this, the spectral data collected from each of the muscles was scaled so that the energy at the higher frequencies matched the energy at the higher frequencies for the normal condition. This was an attempt to match the levels of muscle contraction. Then, the voltage data was compared for all conditions in the beta frequency (24 Hz) band. The results of this comparison for all subjects are shown in Figure 2.b.iii.2. The data is this figure is normalized to the voltage for the cursor movement. As can be seen from the graph, the muscles can only account for 20 to 40 % of the total energy in the beta band under the normal cursor movement conditions, and this is assuming that the subject is not generating an EEG response to the appearance of the targets. The higher values seen with the corrugator and platysma muscle activations are believed to be due to the difficulty in selectively activating these muscles. With the movement of these muscles, it is very likely that the other muscles of facial expression are involved. Based on this data, and on the topographical data that

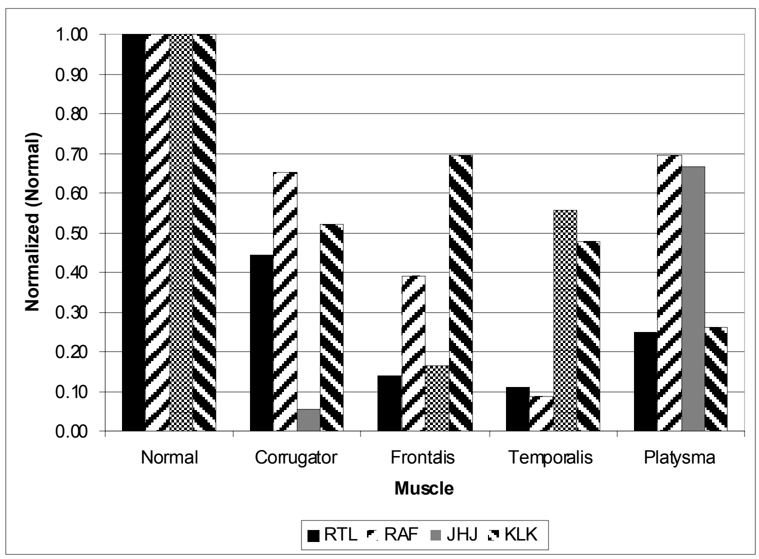

Figure 2.b.iii.2 - Voltage Comparison of Scaled Data

has been presented in previous reports, it is believed that this signal is a cortical signal with some minor EMG contamination.

Plans for Next Quarter

During the next quarter, an attempt will be made to recruit additional neuroprosthesis users for participation this study. Also, hardware and software modification of the BCI system to neuroprosthesis interface will continue so that data collection, signal processing, and command-control computation can be accomplished on one computer. With this accomplished, qualitative and quantitative assessment of the new controller will begin.

Appendix

During this quarter, the work on the EEG-based controller for the hand grasp neuroprosthesis was presented at the First International Conference on Brain-Computer Interface Technology. The presentation was been developed into a short communication article that will be published in a future issue in IEEE Transactions on Rehabilitation Engineering. An abstract of this article is presented below.

"Applications of Cortical Signals to Neuroprosthetic Control: A Critical Review" by RT Lauer, PH Peckham, KL Kilgore and WJ Heetderks.

> The hand grasp neuroprosthesis is a valuable tool for the restoration of hand function in individuals with a cervical level spinal cord injury. The current system, however, has some limitations in how it is controlled which would limit its applications to a broader user population. Future advances in the controller are being developed which would provide for operation that is more natural and that employs fully implantable techniques. One possible controller would employ the use of the electroencephalographic (EEG) signal. Early results indicate that EEG-based control is possible, and may have a potential role in future developments of the neuroprosthesis.

2. b. iv CONTROL OF HAND AND WRIST

Abstract

We are specifying and developing hardware and software to implement both a laboratory and a portable neuroprosthesis for feedforward neural network control of hand grasp and wrist angle. We are currently evaluating the suitability of operating systems and commercial software packages to reduce the design/implementation time required to implement novel systems.

Purpose

The goal of this project is to design control systems to restore independent voluntary control of wrist position and grasp force in C5 and weak C6 tetraplegic individuals. The proposed method of wrist command control is a model of how control might be achieved at other joints in the upper extremity as well. A weak but voluntarily controlled muscle (a wrist extensor in this case) will provide a command signal to control a stimulated paralyzed synergist, thus effectively amplifying the joint torque generated by the voluntarily controlled muscle. We will design control systems to compensate for interactions between wrist and hand control. These are important control issues for restoring proximal function, where there are interactions between stimulated and voluntarily controlled muscles, and multiple joints must be controlled with multijoint muscles.

Progress Report

The neural network feedforward control system that was designed and tested for simultaneous control of hand grasp and wrist position can not be implemented in the neuroprosthesis that is used clinically, and we do not have currently a laboratory system that can implement it. During the last quarter, we specified the hardware and software that will be required to implement the system both in the lab, and in a portable neuroprosthesis. Our current plan is to have a laboratory system□by the end of the current contract. We do not expect to have a portable system within the time frame of this contract, but we expect to have mimicked a portable system in the laboratory.

The requirements of the laboratory system are the following:

1) stimulate all the hand and wrist muscles involved in either grasp mode (lateral or palmar) via either the IRS-8 or IST-10 implantable systems

2) measure via sensors, wrist flexion/extension angle, forearm orientation in the gravitational field, hand grasp opening and hand grasp force

3) compute input/output data sets from steady-state sensor data during constant stimulation with a range of stimulus parameters and combinations of parameters

4) train neural networks with the input/output data

5) implement feedforward control systems for real-time control of hand grasp and wrist angle

6) with the same sensors, measure performance during real-time control

We have begun implementing a laboratory system consisting of a laboratory computer controlling an output stimulus module via a serial interface to an RF stimulator board. All stimulus train control (pulse width, amplitude, and stimulus period on each channel) will be the responsibility of the laboratory computer. This will minimize the hardware development effort in order to start these experiments. We also envision taking maximal advantage of commercially available software (e.g. LabVIEW® and MATLAB®, including the Neural Network Toolbox®) to implement the control systems.

Our principle real-time criterion is that we must communicate with our stimulus module via a serial interface with a repeatable and small latency (on the order of 1-2 ms). During this quarter, we began testing Windows NT® as a possible operating system environment for hosting the real-time control system.

To date, we have installed Windows NT in a computer purchased for this project. This computer also has a National Instruments data acquisition board that can sample the sensors to be used in the control system. We implemented a test program in LabVIEW consisting of the following steps, with a real-time clock in the data acquisition board initiating the A/D sampling and stimulus period.

1. Sample analog signals via the A/D
2. Perform some simple arithmetic operation on the analog signals
3. Calculate the stimulus parameters for 10 channels of stimulation
4. Transmit the stimulator control data to the RF output board via a serial port running at 38.4 K bits/sec
5. Return to step 1

This sequence is the basic outline of a feedforward control system for hand and wrist control. This test program, written in LabVIEW, ran successfully at a stimulus frequency of 20 Hz determined by the real-time clock (stimulus period of 50 ms). In addition, the CPU overhead for this process was only approximately 30 ms, leaving the remaining 20 ms for more complicated neural-network calculations.

One scenario is to use LABVIEW for the basic stimulation and data collection control, but link to a MATLAB trained and compiled subroutine to perform the neural network calculations.

Plans for next quarter

We will continue to develop hardware and software specifications, as well as test the capabilities of the commercially available software. We expect to choose an operating system and begin developing software in this quarter.